Graphene quality evaluation by Van der Pauw-Hall Method

Chunlin Liu [1, 2, *]

[1]National Key Laboratory of Electronic Thin Films and Integrated Devices, University of Electronic Science and Technology of China, Chengdu, 610054, China

[2]School of Integrated Circuit Science and Engineering, University of Electronic Science and Technology of China, Chengdu, 610054, China

* liuchunlin@std.uestc.edu.cn

Abstract. Evaluating graphene quality is crucial for both industrial applications and academic research. Traditional methods like Optical Microscope, Raman Spectroscope, Scanning and Transmission Electron Microscope, while common, face challenges in convience and providing electrical performance. To address these limitations, a cost-effective and rapid method was introduced for assessing macroscopic quality of graphene. This technique involves fine-tuning carrier concentration over 1013 cm-2 by controlling hydrochloric acid (HCl) doping time. Utilizing the Van der Pauw-Hall system, it tracks carrier concentration changes of graphene, allowing for mobility measurement under consistent carrier conditions. This facilitates a direct comparison of different graphene samples. The method shows reproducibility in evaluating HCl-doped graphene, which is consistent with the Raman characterizations. This advancement in graphene evaluation, focusing on mobility comparison at identical carrier concentrations, sets the stage for standardized assessments in the graphene industry.

Keywords: graphene, quality, evaluation, Van der Pauw-Hall (VDP-H), hydrochloric acid (HCl)

1. Introduction

Since the discovery of graphene through mechanical exfoliation in 2004,[1] the landscape of research across diverse fields has been profoundly impacted. Graphene applications span from photodetectors and mechanical sensors to biosensors and new energy evolution.[2-4] Particularly noteworthy is the discovery of magic angle graphene, a breakthrough in superconductivity, deepening the state-of-the-art research and signaling a bright future for graphene.[5] The chemical vapor deposition (CVD) synthesis of graphene in 2009 is marked a significant milestone,[6] expanding its utility in academic research and potential in industrial applications, thereby ushering in the era of graphene as a "star material". In recent years, inspiring advancements, such as the synthesis of wafer-scale graphene single crystals and superclean graphene,[7-9] all contribute to the rapid pace of industrial development. However, these advancements also highlight the challenges in graphene characterization. The methods employed are diverse, generally expensive, time-consuming, and complicated. For instance, to underscore graphene high quality, some studies have extracted its mobility by fabricating thin flm transistors (TFT) at the micro/nano scale.[10-13] This approach, while innovative, results in varying mobility readings due to different area data used in the same TFT transfer characteristic curve. More important, the device fabrication process is cumbersome, time-consuming, and high-cost. Such micro-region results do not accurately represent the quality of graphene at a macro scale.

The mobility of devices made from graphene is not solely dependent on the crystal structure of the material but is also significantly influenced by the substrate, device fabrication process, and the measurement environment.[7, 14] Achieving consistency in these areas is challenging and directly impacts the accuracy of graphene evaluation. Conventional characterization methods have their drawbacks. Optical microscope (OM), for instance, can only assess the continuity of graphene, not its overall quality.[15] Scanning electron microscope (SEM), though insightful, involves a cumbersome and expensive process.[16] Raman spectroscope offers detailed defect analysis but is limited to small-scale regions and becomes time-intensive when conducting mapping studies.[17]

In light of these limitations, there is a pressing need for a simpler, faster, and more cost-effective method to evaluate the quality of different graphene samples. Such a method would revolutionize the standard for graphene characterization, making it more accessible and consistent. It would allow for a better understanding of graphene properties and its suitability for various applications, aligning academic research more closely with industrial needs. This need for a new approach to graphene characterization is a call to action for researchers and industry professionals alike, to develop innovative techniques that can provide a more comprehensive and accurate assessment of graphene properties. The development of such a method will be crucial in realizing the full potential of graphene in various applications, from electronics to energy solutions.

2. Experimental section

2.1 Materials

Graphene was synthesized by CVD method, and it was transferred onto 285 nm thick SiO2/Si substrate by Poly (methyl methacrylate) assisted. The dopants used in the process included hydrochloric acid (HCl; CAS No. 7647-01-0) and nitric acid (HNO3; CAS No. 7697-37-2), sourced from Chengdu Chron Chemicals, and chloroauric acid (HAuCl4; CAS No. 16961-25-4) and ferric chloride (FeCl3; CAS No. 10025-75-1), produced from Sigma-Aldrich and Shanghai Aladdin Biochemical Technology, respectively.

2.2 Sample treatment

In the doping process, graphene samples were doped using natural volatile vapors from solutions of HCl and HNO3, by positioning the graphene 2 cm above the solutions. For HAuCl4 (80 mM) and FeCl3 (1 M) doping, the solutions were spin-coated onto the graphene surface at 3000 rpm for 30 seconds. Four laboratory reagents were selected for their simplicity, speed, and cost-effectiveness as dopants: HCl, HNO3, HAuCl4, and FeCl3. Eight graphene samples (S1-S8) from the same batch were doped with these four dopants. Samples S1-S2, S3-S4, S5-S6, and S7-S8 were doped with HCl, HNO3, HAuCl4, and FeCl3, respectively. To compare, samples S1, S3, S5, and S7 underwent additional ultraviolet (UV) light irradiation post-doping to expedite dopant desorption from the graphene surface. The Van der Pauw-Hall (VDP-H) test system was used to determine basic electrical parameters like carrier concentration (n), mobility (μ), and sheet resistance (R). This system allows for successive parameter measurement with a 23-second interval between consecutive results.

2.3 Characterizations.

The following equipment was used: OM (Nikon, ECLIPSE LV100D), SEM (Navo NanoSEM450), Raman spectroscope (Renishaw Invia, equipped with 532 nm laser), X-ray photoelectron spectroscopy (XPS; Kratos-Axis Supra, K-Alpha) and Van der Pauw-Hall measurement (VDP-H; Ecopia, HMS-5000). UV irradiation was achieved by UV light (Shenyu, UV-A 365 nm).

3. Results and discussion

Fig. 1(a) illustrates the changes in carrier concentration (n) of graphene over time, both with and without UV irradiation. For graphene doped with HCl and HNO3, n can be as high as 1013 cm-2. However, for samples doped with HAuCl4 and FeCl3, n significantly exceeds 1013 cm-2, showing negligible change within 40 minutes in the absence of UV irradiation, which generate photoinduced molecular desorption.[18] Notably, the doping of graphene with HNO3 results in a significant reduction in n, dropping from 1013 cm-2 to 8.3×1012 cm-2, with HCl-doped samples showing a subsequent decrease. The n is further diminished under UV irradiation across all samples, with HCl-doped graphene experiencing a notable decrease from 1013 cm-2 to 7.2×1012 cm-2. In

contrast, HNO3 doping can rapidly increase n to over 1013 cm-2 within seconds, highlighting its poor controllability due to the challenge of regulating n through doping duration. HAuCl4-doped graphene exhibits significant variability under UV exposure, yet maintains a high doping level, failing to reach 1013 cm-2 even after 40 minutes. Meanwhile, FeCl3 doping, while altering n, yields inconsistent results under the same conditions, rendering it an unreliable method for achieving stable and controllable doping. Fig. 1(b) shows that doping with HAuCl4 and FeCl3 leads to strong fluctuations in graphene, likely due to the high doping levels and environmental noise influences. Additionally, HNO3, known for its corrosive and strong oxidizing properties, not only presents safety hazards but also introduced inconsistencies in doping as shown in Fig. 1, making it an unsuitable candidade for atmospheric experiments. Similarly, HAuCl4 is quite expensive, susceptible to light-induced decomposition, and exhibits stable high doping level with both corrosive and toxic properties.[19] In other words, HCl stands out as a dopant that is stable, controllable, and cost-effective among the options considered.

Research indicates that the μ-n correlation of monolayer graphene on SiO2 substrates can be fitted with a power exponent function. The absolute values of the exponent |α| for S1-S4 samples are 0.44, 0.47, 0.49, and 0.52 respectively, aligning with previous report.[20] However, the carrier concentration and mobility of HAuCl4 and FeCl3 doped graphene in air exhibit significant fluctuations, leading to inconsistencies in the μ-n correlation of graphene as compared to the reported data.[20]

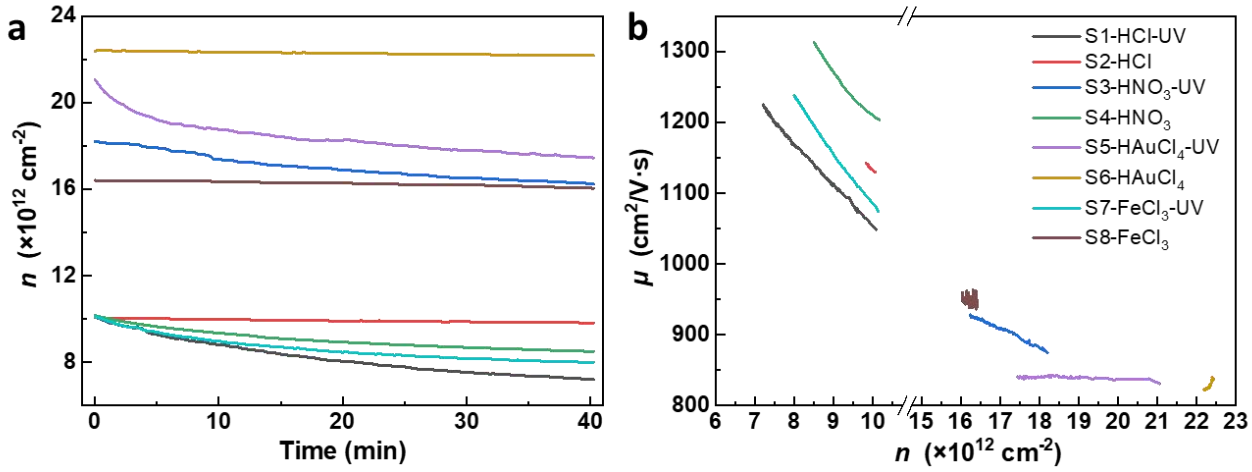

Fig. 1. VDP-H methods characterization of graphene (S1-S8) after dopant treatment.
(a) Carrier concentration (n) v.s. time
(b) the corresponding relationship between carrier mobility (μ) and carrier concentration (n).

To assess the impact of various dopants on the properties of graphene, XPS characterization was employed, with the results depicted in Fig. 2. The XPS wide-scan spectra in Fig. 2(e) reveal characteristic peaks associated with graphene doped with four distinct dopants, in comparison to undoped graphene. Upon transferring the graphene onto a SiO2 substrate, peaks corresponding to Si 2p and O 1s were detected, indicative of the substrate's composition. Notably, the presence of hypochlorite and other chlorine-containing functional groups, typically found in chlorinated water, led to the identification of Cl 2p peaks, albeit in small quantities. A detailed examination of the fine structure spectroscope in HCl-doped graphene, as shown in Fig. 2(a), revealed a prominent Cl 2p peak. It should be noted that the Cl 2p peak in undoped graphene is likely due to the presence of water or etching solution from the transfer process. In the case of HNO3 doping, Fig. 2(b) displays a pronounced N 1s peak in the HNO3-doped graphene, while the N 1s peak in undoped graphene is attributed to atmospheric nitrogen. For HAuCl4-doped graphene, Fig. 2(c) shows a distinct Au 4f peak, indicating two chemical environments for Au due to the photolysis property of HAuCl4, which causes peak splitting from partial decomposition, thus confirming effective doping. Finally, the Fe 2p peak in Fig. 2(d) confirms the successful doping of graphene with FeCl3. The

comprehensive XPS analysis thus validates the successful incorporation of the aforementioned dopants into the graphene structure.

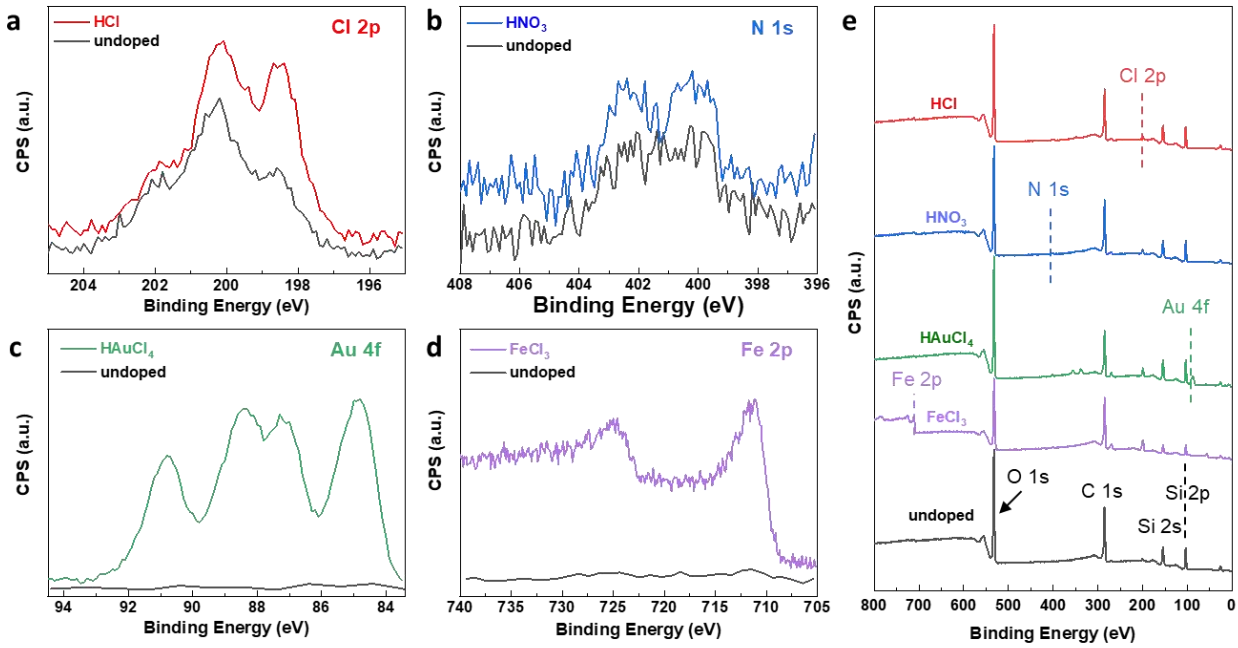

Fig. 2. XPS characterization of graphene on SiO2 substrate. Fine structure spectra of (a) Cl 2p (HCl doped), (b) N 1s (HNO3 doped), (c) Au 4f (HAuCl4 doped) and (d) Fe 2p (FeCl3 doped) graphene. (e) Wide spectra of graphene doped with HCl, HNO3, HAuCl4, FeCl3 and undoped as-transferred graphene on SiO2 substrate.

To evaluate the integrity of graphene at similar doping levels, the effects of HCl doping were examined. These findings, as depicted in Fig. 3, indicate that the graphene's continuity is preserved after 60 seconds of HCl doping, supported by OM and SEM images in Fig 3(a) and 3(d), respectively. The OM images clearly display the continuous fold lines of graphene wrinkles, while the SEM images show a relatively clean surface with minimal debris. Raman spectra, presented in Fig. 3(b) and 3(e), confirms a low defect density in the graphene and an increase in carrier concentration, evidenced by the enhanced ratio of the 2D peak intensity to the G peak intensity (I_{2D}/I_G) following HCl doping. [17] Additionally, VDP-H results, as shown in Fig. 3(c), demonstrate that the carrier concentration is significantly affected by the duration of HCl exposure. Within 60 seconds, a notable increase in carrier concentration is observed, surpassing 10^{13} cm^{-2}. This suggests that there is an adequate time window to achieve precise control over the carrier concentration around 10^{13} cm^{-2} using HCl doping, highlighting its controllable nature. However, it is crucial to recognize that while the general trend of HCl doping is consistent across different graphene samples, individual doping profiles may differ due to varying initial doping levels. Raman statistical analysis in Fig. 3(f) shows a low doping level (~2.3×10^{12} cm^{-2}) without HCl doping, which is contrasted by a substantial increase to 10^{13} cm^{-2} after 60 seconds of HCl exposure. The congruence between the Raman and VDP-H characterization supports the efficacy of HCl as a dopant.[21] This establishes the potential for uniform doping of graphene using HCl, laying the groundwork for achieving consistent doping at a standardized level.

Validating the universality of HCl doping for evaluating graphene quality, four monolayer graphene samples (G1-G4) were treated with HCl. The results, as presented in Fig. 4, show the evolution of graphene properties after HCl application. Over the course of 300 minutes following post-treatment, the *n* of the samples decreased, as indicated in Fig. 4(a). Mobility experienced a slight increase over time, as shown in Fig. 4(c), while sheet resistance showed subtle variations, aligning with Ohm's law, [20] as depicted in Fig. 4(b). The relationship between mobility and carrier concentration is represented by the power exponent function in Fig. 4(d). These changes in

carrier concentration post-HCl doping highlight the dopant's effectiveness in regulating graphene's carrier concentration. This regulation allows for a standardized comparison of carrier concentrations across different graphene samples, ensuring a more uniform and consistent evaluation of graphene quality.

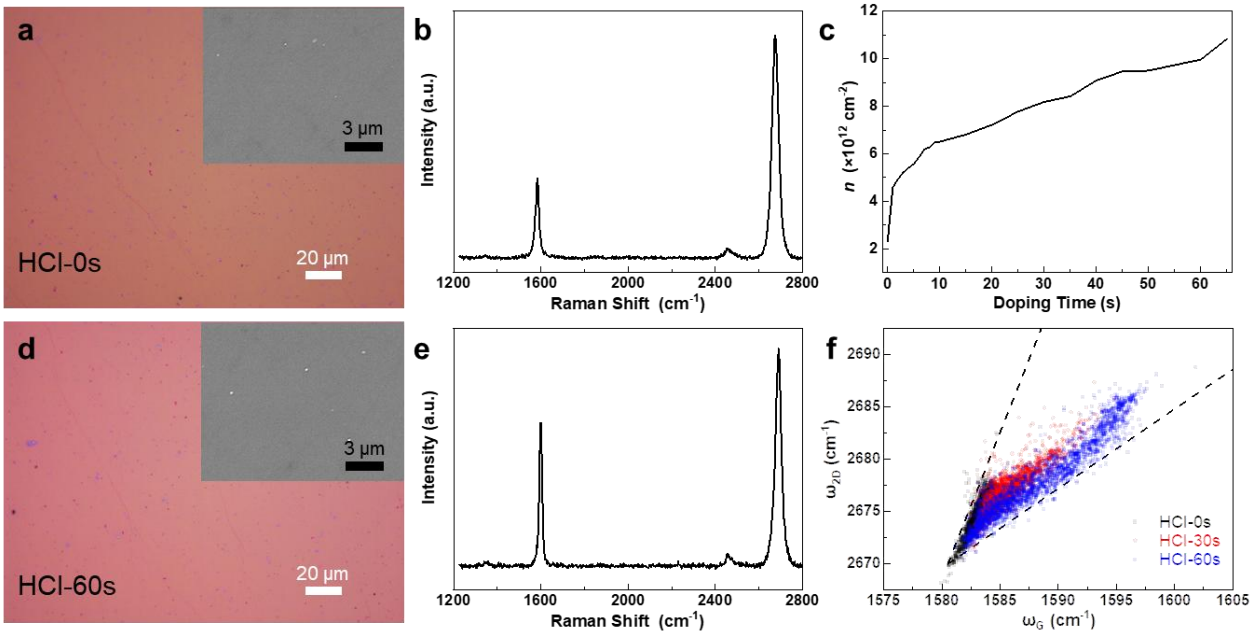

Fig. 3. OM/Raman characterization of graphene film before (a)/(b) and after (d)/(e) HCl doped for 60s, the corresponding inserts in OM are typical SEM image.
(c) graphene carrier concentration and (f) correlation between 2D and G band frequencies (the upper and lower black dashed line marks the strain and doping limit, respectively) of graphene (ω2D, ωG) with different HCl doping time.

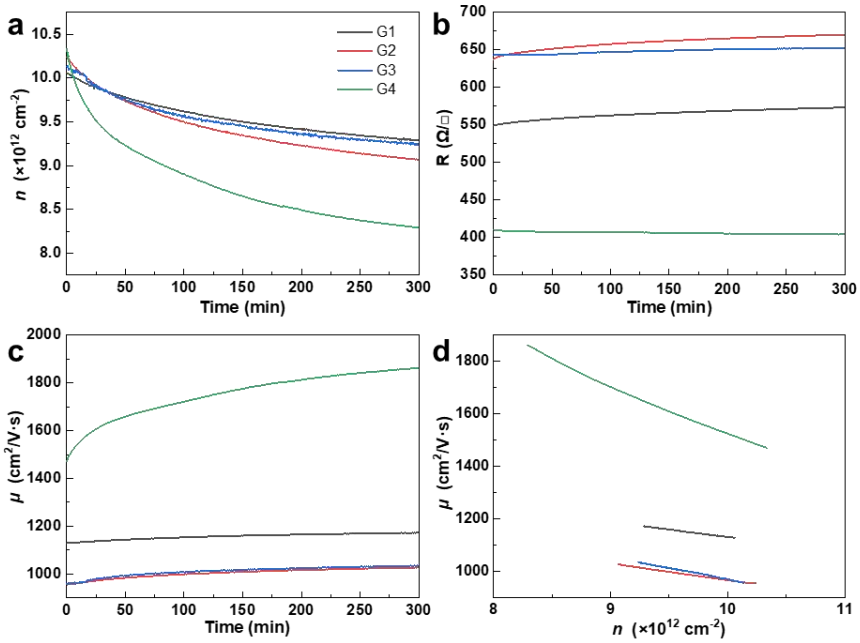

Fig. 4. Hall characteriazation of four graphene samples (G1-G4) after HCl doping.
(a) carrier concentration (n), (b) sheet resistance (R), (c) mobility μ v.s. time and (d) μ v.s. n.

4. Summary

In general, this study introduces a mechanical damage-free method for doping graphene with HCl vapor, significantly simplifying the evaluation of macro-scale graphene quality. This straightforward graphene quality assessment approach overcomes the traditionally time-consuming, cumbersome, and costly challenges. By doping graphene with HCl, key electrical parameters like carrier concentration, mobility, and sheet resistance can be swiftly and precisely determined using VDP-H measurement. This technique offers a dependable foundation for evaluating graphene suitability for industrial applications, streamlining the process and enhancing its practicality.

References

[1] Geim, Andre K.; Novoselov, Konstantin S., The rise of graphene. Nat. Mater., 2007, 6(3): 183-191.

[2] Schuler, Simone; Schall, Daniel; Neumaier, Daniel, et al., Graphene photodetector integrated on a photonic crystal defect waveguide. ACS Photonics, 2018, 5(12): 4758-4763.

[3] Yu, Rufang; Zhu, Chengyan; Wan, Junmin, et al., Review of graphene-based textile strain sensors, with emphasis on structure activity relationship. Polymers, 2021, 13(1): 151.

[4] Hwang, Michael Taeyoung; Heiranian, Mohammad; Kim, Yerim, et al., Ultrasensitive detection of nucleic acids using deformed graphene channel field effect biosensors. Nat. Commun., 2020, 11(1): 1543.

[5] Cao, Yuan; Fatemi, Valla; Fang, Shiang, et al., Unconventional superconductivity in magic-angle graphene superlattices. Nature, 2018, 556(7699): 43-50.

[6] Li, Xuesong; Cai, Weiwei; An, Jinho, et al., Large-area synthesis of high-quality and uniform graphene films on copper foils. Science, 2009, 324(5932): 1312-1314.

[7] Li, Junzhu; Chen, Mingguang; Samad, Abdus, et al., Wafer-scale single-crystal monolayer graphene grown on sapphire substrate. Nat. Mater., 2022, 21(7): 740-747.

[8] Zhang, Jincan; Sun, Luzhao; Jia, Kaicheng, et al., New growth frontier: superclean graphene. ACS Nano, 2020, 14(9): 10796-10803.

[9] Zhang, Jincan; ha, Kaicheng; Lin, Li, et al., Large-area synthesis of superclean graphene via selective etching of amorphous carbon with carbon dioxide. Angew. Chem., Int. Ed., 2019, 58(41): 14446-14451.

[10] Lemme, Max C.; Echtermeyer, Tim J.; Baus, Matthias, et al., A graphene field-effect device. IEEE Electron Device Lett., 2007, 28(4): 282-284.

[11] Roy, T.; Hesabi, Z. R.; Joiner, C. A., et al., Barrier engineering for double layer CVD graphene tunnel FETs. Microelectron. Eng., 2013, 109: 117-119.

[12] Zhong, Hua; Zhang, Zhiyong; Xu, Haitao, et al., Comparison of mobility extraction methods based on field-effect measurements for graphene. AIP Adv., 2015, 5(5): 057136.

[13] Sque, Stephen J.; Jones, Robert; Briddon, Patrick R., The transfer doping of graphite and graphene. Phys. Status Solidi A, 2007, 204(9): 3078-3084.

[14] Takahashi, N.; Watanabe, K.; Taniguchi, T., et al., Atomic layer deposition of Y_2O_3 on h-BN for a stack in graphene FETs. Nanotechnology, 2015, 26(17): 175708.

[15] Roddaro, S.; Pingue, P.; Piazza, V., et al., The optical visibility of graphene: Interference colors of ultrathin graphite on SiO_2. Nano Lett., 2007, 7(9): 2707-2710.

[16] Zan, Recep; Muryn, Chris; Bangert, Ursel, et al., Scanning tunnelling microscopy of suspended graphene. Nanoscale, 2012, 4(10): 3065-3068.

[17] Das, A.; Pisana, S.; Chakraborty, B., et al., Monitoring dopants by Raman scattering in an electrochemically top-gated graphene transistor. Nat. Nanotechnol., 2008, 3(4): 210-215.

[18] Sun, Pengzhan; Zhu, Miao; Wang, Kunlin, et al., Photoinduced molecular desorption from graphene films. Appl. Phys. Lett., 2012, 101(5): 053107.

[19] Chen, Ming; Wang, DaMeng; Liu, XiangDong, Direct synthesis of size-tailored bimetallic Ag/Au nano-spheres and nano-chains with controllable compositions by laser ablation of silver plate in $HAuCl_4$ solution. RSC Adv., 2016, 6(12): 9549-9553.
[20] Qing, Fangzhu; Shu, Yang; Qing, Linsen, et al., A general and simple method for evaluating the electrical transport performance of graphene by the van der Pauw-Hall measurement. Sci. Bull., 2018, 63(22): 1521-1526.
[21] Lee, Ji Eun; Ahn, Gwanghyun; Shim, Jihye, et al., Optical separation of mechanical strain from charge doping in graphene. Nat. Commun., 2012, 3: 1024.